Channel Estimation on MIMO-OFDM Systems

André Antônio dos Anjos
Instituto Nacional de Telecomunicações
Av. João de Camargo, 510 - 37540-000
Santa Rita do Sapucaí - MG - Brazil
andre-anjos@inatel.br

Ricardo Antonio Dias
Instituto Nacional de Telecomunicações
Av. João de Camargo, 510 - 37540-000
Santa Rita do Sapucaí - MG - Brazil
radias@inatel.br

Luciano Leonel Mendes
Instituto Nacional de Telecomunicações
Av. João de Camargo, 510 - 37540-000
Santa Rita do Sapucaí - MG - Brazil
lucianol@inatel.br

Abstract— **Modern mobile telecommunication systems are using MIMO combined with OFDM, which is known as MIMO-OFDM, to provide robustness and higher spectrum efficiency. One major challenge in this scenario is to obtain an accurate channel estimation to detect the information symbols, once the receiver must have the channel state information to equalize and process the received signal. The main goal of this paper is to present some techniques and analysis for channel estimation in MIMO-OFDM systems, considering the influence of various system parameters on the channel estimation error and on the final system performance.**

Index Terms— **MIMO-OFDM, OFDM, channel estimation, diversity.**

I. Introduction

Nowadays, telecommunication services demand high data rates with reliability. However, to achieve high data rates it is necessary to use a wide spectral bandwith, which makes the system economically unfeasible. Another problem is that, in this scenario, the channel becomes very selective [1], impairing the reliability of the received information. In order to minimize these problems, digital signal processing techniques combined with designing transceivers strategies are used, where Multiple Inputs and Multiple Outputs (MIMO) deserves mention. MIMO systems use multiple antennas to transmit and multiple antennas to receive signals [2][3]. The multiple signals transmitted and the multiples replicas obtained in the receiver can be combined to increase the robustness (diversity) or the data rate (multiplexing).

Orthogonal Frequency Division Multiplexing technique (OFDM) [4] are commonly used to overcome the ISI (Inter Symbol Interference) introduced by multipath channel. This technique is employed in several digital communications standards, such as DVB-T (Digital Video Broadcasting - Terrestrial), DVB-T2, ISDB-T (Integrated Services Digital Broadcasting - Terrestrial), WiFi, Wi-Max (Worldwide Interoperability for Microwave Access), LTE (Long Term Evolution), and others.

Therefore, future telecommunication systems tend to combine both techniques mentioned above, known as MIMO-OFDM systems [2][3]. Depending on the designed scheme, a system operating with MIMO-OFDM can provide robustness against frequency-selective and time-variant channels, and/or to obtain multiplexing gain. The major challenge in this scenario is to obtain accurate channel estimation for detection of the information symbols, since the receiver requires the

Channel State Information (CSI) to equalize the received symbols, due to the phase rotation and amplitude attenuation caused by the channel [5].

The main goal of this paper is to present an analysis for channel estimation in MIMO-OFDM scheme. A comparison is made between the presented estimation techniques, showing the advantages and disadvantages of each one. The influence of various system parameters on the channel estimation error and in the final performance of the system will also be evaluated. All tests will be conducted using the MATLAB. Root-mean-square-error method is used to measure the deviation between the actual and estimated channel. Another parameter that will be used to analyze the systems performance is the MER (Modulation Error Rate), which measures the dispersion of the constellation of the received symbols.

This paper is organized as follows: Sections II and III provide basics concepts of MIMO and OFDM techniques, respectively. Section IV presents some methods to perform the channel estimation in MIMO-OFDM systems. Then, in Section V, the results of the simulations are presented. Finally, in Section VI brings the final conclusions of the paper.

II. MIMO Systems

MIMO systems [6] use multiple antennas in the transmitter ande receiver sides. The signals sent by the transmitter antennas are received by the receiver antennas and then combined, in order to achieve a reduction of the bit error rate (BER) or a capacity gain. Figure 1 shows a block diagram of a basic MIMO system.
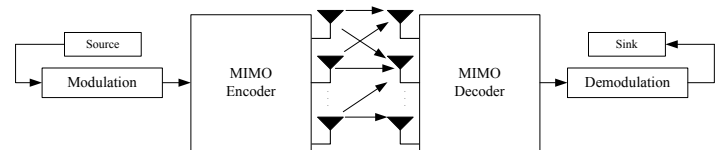

Fig. 1. Block diagram of a basic MIMO system.

Taking advantage of what the MIMO technique can provide, three features stand out: (a) diversity gain, (b) multiplexing gain or (c) both gains. These features are explored in the following subsections.

A. Diversity gain in MIMO systems

MIMO technique for diversity gain [7] takes advantage of the signals arriving at the receiver by multiple channels. These

signals can be combined constructively at the receiver side, i.e., in a favorable way to estimate the information transmitted. It is possible to take advantage of temporal diversity or frequency diversity combined with space diversity. Figure 2 shows an example of MIMO system for diversity gain, where h_{ij} represents the channel gain between the i-th transmitter antenna and the j-th receiver antenna.
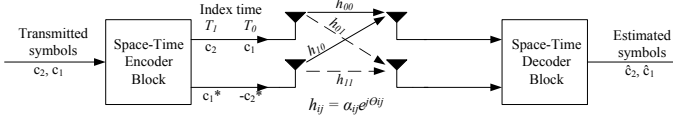

Fig. 2.   Block diagram of a MIMO system for diversity gain.

B. Multiplexing Gain in MIMO Systems

MIMO systems can also be used to provide multiplexing gain [8], which increases the system capacity, because different symbols are transmitted by different antennas at the same time. Since the channel between each transmission and reception antenna will be unique, each transmitted symbol can be recovered through digital signal processing. Zero-Forcing technique is commonly used to recover the data symbols from the received signals. Figure 3 illustrate a MIMO system for multiplexing gain.
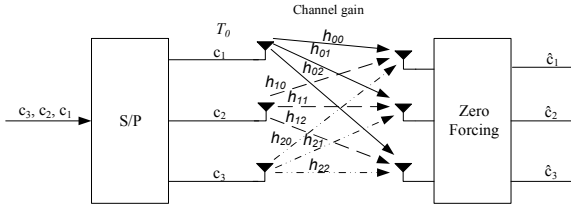

Fig. 3.   Block diagram of a MIMO system for multiplexing gain.

C. Hybrid MIMO

The two features mentioned in the previous subsections can be used together. This type of system is called hybrid MIMO system [9]. In this scheme, a committed relationship should be taken into account, where a higher multiplexing gain implies in less diversity gain and vice-versa. Figure 4 illustrate a possible use of this hybrid technique, where a 3×3 MIMO is used to achieve a spectrum efficiency of $4/6 = 2/3$ of the maximum that can be obtained and where two symbols (C_1 and C_2) are received with diversity gain of order 6.
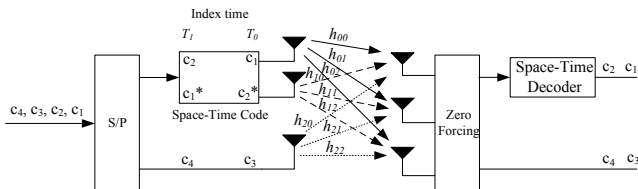

Fig. 4.   Block diagram of a hybrid MIMO.

III. OFDM SYSTEMS

The OFDM system [5] is based on the transmission of complex symbols using N orthogonal subcarriers. The serial high data-rate stream is converted into N low data-rate sub-streams. In this system, if the number of subcarriers is large enough, the channel frequency response for a single subcarrier may be considered to be flat. Since the subcarriers can be individually demodulated, OFDM provides a higher robustness to the transmitted data. Figure 5 shows the block diagram of the OFDM scheme.
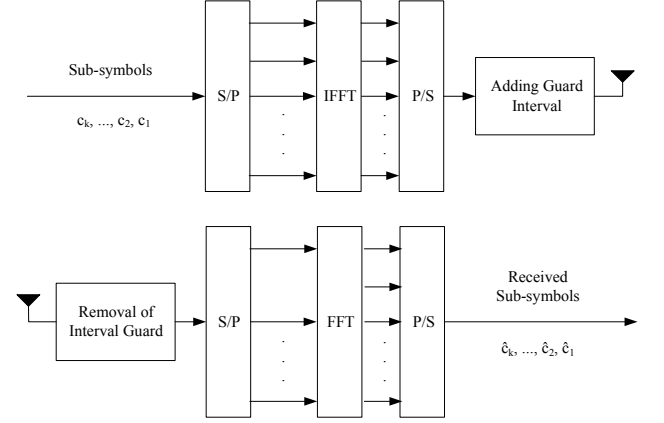

Fig. 5.   Block diagram of an OFDM system.

In OFDM systems, the transmitted symbols are separated by a time guard interval that improves the performance of the system. The addition of this extra interval is performed by copying the end of the OFDM symbol at its beginning. The purpose of the guard interval is to introduce robustness against multipath channels [10].

IV. CHANNEL ESTIMATION FOR MIMO-OFDM SYSTEMS

The combination of MIMO and OFDM has become very attractive for broadband communication systems, because of the individual characteristics of each technique. Figure 6 shows a simplified MIMO-OFDM system [11][12].

Due to the multipath channel, each OFDM subcarrier is affected by attenuation and a phase rotation. To receive the symbols correctly, the receiver must be able to estimate the channel frequency response. In wireless systems, three methods are commonly used to estimate the channel [13][14], and they are explained in the next subsections.

A. Channel Estimation using pilot symbols

In this type of estimation, all subcarriers of a specific OFDM symbol carry reference data that are known a priori by the receiver. This estimation method provides a perfect channel estimation during the pilot symbol [15], if the noise is disregarded. However, since a new pilot symbol must be sent within the channel coherence time, this solution can only be used in slow fading channels. In this case, several data symbol can be transmitted between two pilot symbols, reducing the impact of the pilot symbols in the system throughput. The
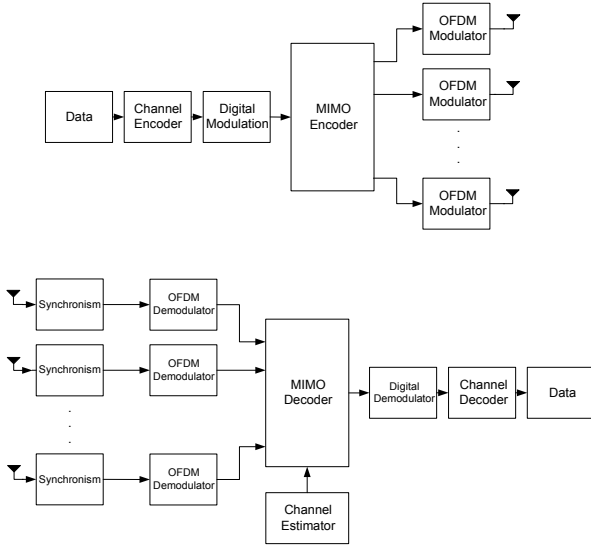
Fig. 6.   Block diagram of a MIMO-OFDM system.

throughput of a OFDM system using pilot symbols is given by

$$R_b = \frac{K_D}{K_D + 1} \times \frac{N \log_2(M)}{T_{OFDM}}, \quad (1)$$

where K_D is the number of OFDM data symbols transmitted between two data symbols, N is the number of subcarriers of an OFDM symbol, M is the modulation order and T_{OFDM} is the time duration of one OFDM symbol. This type of estimation is ideal for highly frequency-selective channels with a large coherence time.

B. Channel estimation using pilot subcarriers

In this case, the estimation is performed by sending frequency-spaced pilots in all transmitted OFDM symbols [15][16]. The smaller the frequency distance between the pilots, the better is the channel estimation. However, a larger the number of pilots subcarries, will lead to a prohibitive reduction in the data rate. The throughput, in this case, is given by

$$R_b = (N - N_P) \times \frac{\log_2(M)}{T_{OFDM}}, \quad (2)$$

where N_P represents the number of pilot subcarriers. This type of channel estimation is ideal for faster and less frequency selective channels. Most of the analysis performed in Section V use this method of estimation, because it is widely employed by the digital communication standards.

C. Hybrid channel estimation

The hybrid estimation is a combination of the two techniques mentioned previously, where symbols containing only pilots (pilot symbols), and symbols containing data subcarriers interspersed with pilot subcarriers are used. Thus, an accurate estimation of the channel is held every K_D OFDM symbols. In the remaining time, the estimation is not as precise as the

first one, but enough to maintain a good channel estimation. In this case, the throughput is given by

$$R_b = \frac{K_D}{K_D + 1} \times \frac{(N - N_P) \log_2(M)}{T_{OFDM}}. \quad (3)$$

D. Channels estimation for MIMO-OFDM

The MIMO-OFDM system that will be used in this paper is presented in Figure 7. This scheme is known as STC-OFDM [7][14] (Space Time Code OFDM) and offers a 4-order diversity gain. In this model, if the noise effect is disregarded,
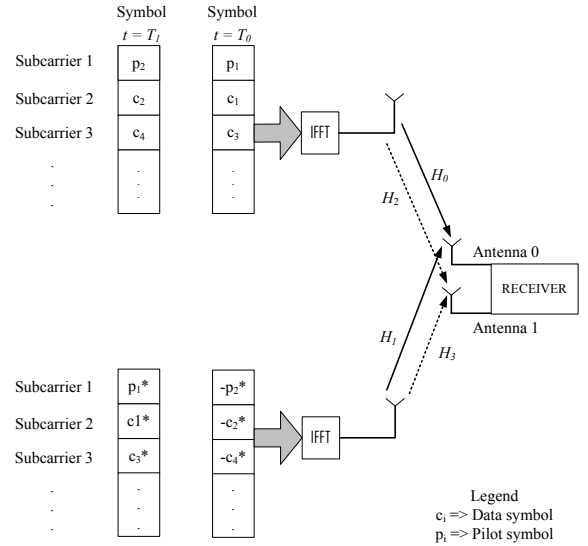

Fig. 7.   MIMO-OFDM system analyzed.

the received signals in pilot subcarriers at the receiving antenna 0 are given by

$$P'[n] = p[n]H_0 - p^*[n+1]H_1, \quad (4)$$

$$P'[n+1] = p[n+1]H_0 + p^*[n]H_1, \quad (5)$$

where $p[n]$ is a pilot subcarrier transmitted at time instant nT_0, $(\cdot)^*$ is the conjugate operation and H_i represents the frequency gain for the i-th channel in the frequency of the pilot subcarrier analyzed. Thus, assuming that the value $p[n] = p[n+1] = p$ and $p \in \Re$ and solving (4) and (5), the channels estimation can be obtained by to

$$H_0' = \frac{P'[n+1] + P'[n]}{2p}, \quad (6)$$

$$H_1' = \frac{P'[n+1] - P'[n]}{2p}. \quad (7)$$

The same analysis can be done to estimate the channels H_2 and H_3, related with the receiving antenna 1. Once obtained the channel estimations at the frequency of the pilot subcarriers, it is then necessary to use some interpolation technique to obtain an estimative of the channel frequency response at the frequency of all data subcarriers. It is important to note that to estimate the channel completely, in the scenario presented in Figure 7, it takes $2 T_{OFDM}$. It means that the channel cannot

vary during this time interval. In other words, the coherence time of the channel must be greater than $2\,T_{OFDM}$.

The root-mean-square error (RMSE) is used to measure the deviation between the actual and estimated channel frequency response. It can be evaluated by

$$E_{CE} = \frac{\sqrt{\sum_{i=0}^{N-1}\left[H[i] - H'[i]\right]^2}}{N}, \qquad (8)$$

where $H'[i]$ is the estimated channel at subcarrier i and N is the number of subcarriers in one OFDM symbol.

Another important parameter that will be used to analyze the performance of systems is the MER (Modulation Error Rate), which measures the dispersion of the constellation of the estimated symbols. Its value is given by

$$MER = \frac{\sum_{n=0}^{N-1}\left[I_n{}^2 + Q_n{}^2\right]}{\sum_{n=0}^{N-1}\left[(I'_n - I_n)^2 + (Q'_n - Q_n)^2\right]}, \qquad (9)$$

where I_n and Q_n represent the in-phase and quadrature components of the n-th transmitted symbol and I'_n and Q'_n represent the in-phase and quadrature components of the received symbol. Usually, this measure is expressed in decibels.

V. Performance Analysis

The main purpose of this section is to analyze the influence of different system parameters on the channel estimation and, consequently, in the final performance of the system. MATLAB has been used to simulate the system presented in Figure 7. The simulation parameters are shown in Table I.

TABLE I

System parameters.

Parameters	Value
Mapping	16-QAM
Total number of subcarriers	8192
Number of pilot subcarriers	257
OFDM symbol duration(T)	1.024 ms
Distance between the pilot subcarriers	31.25 kHz
Modulation employed in the pilot subcarriers	BPSK
Sampling rate	8 MHz

A. Influence of the interpolation method in the channel estimation and system performance

This subsection presents the simulation results about the influence of interpolation method on the quality of the channel estimation. The RMSE of the channel estimation and the MER of the linear, cubic and DFT interpolation methods are evaluated. All three interpolation methods are detailed in [14]. The delay profile for this analysis is presented in Table II.

Using the linear interpolation method to estimate the channel, the RMSE is 3.32×10^{-4}, and the MER is 30.7 [dB]. Figure 8 present the symbol dispersion due to channel estimation error using linear interpolation.

TABLE II

Delay profile of channel 1.

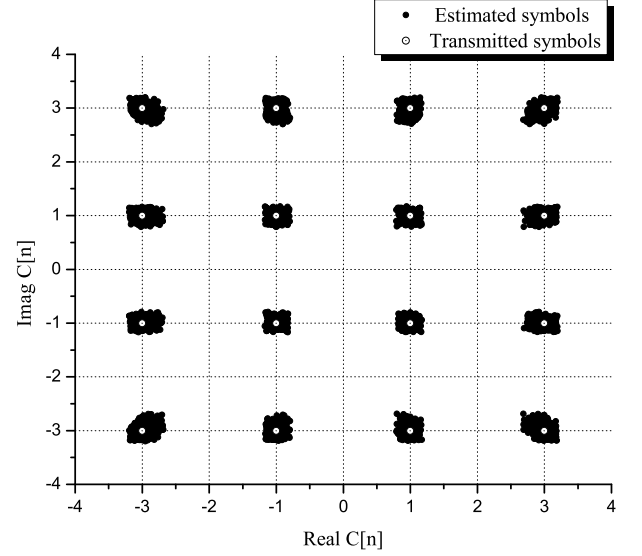| Parameter	P_0	P_1	P_2	P_3	P_4	P_5
Delay [μs]	0	0.15	2.22	3.05	5.86	5.93
Gain [dB]	0	-13.8	-16.2	-14.9	-13.6	-16.4

Fig. 8.   Symbol dispersion using linear interpolation.

It is important to remember that the deviation suffered by the symbol constellation shown in Figure 8 is only due to channel estimation error.

For the cubic interpolation method, the RMSE is 5.063×10^{-5}, resulting in an MER of 47.1 [dB]. Figure 9 shows the received symbols constellation using cubic interpolation to estimate the channel.
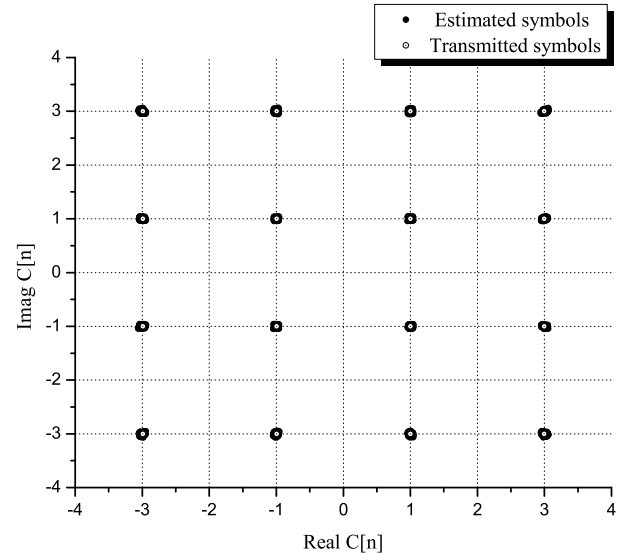

Fig. 9.   Symbol dispersion using cubic interpolation.

The third and final interpolation method analyzed is the DFT

interpolation. With this method, the estimation RMSE is 2.38×10^{-18} and the MER is 310.7 [dB], which is equivalent to say that the deviation of the constellation is practically zero. Figure 10 shows the constellation of the received symbols when the DFT interpolation method is used.
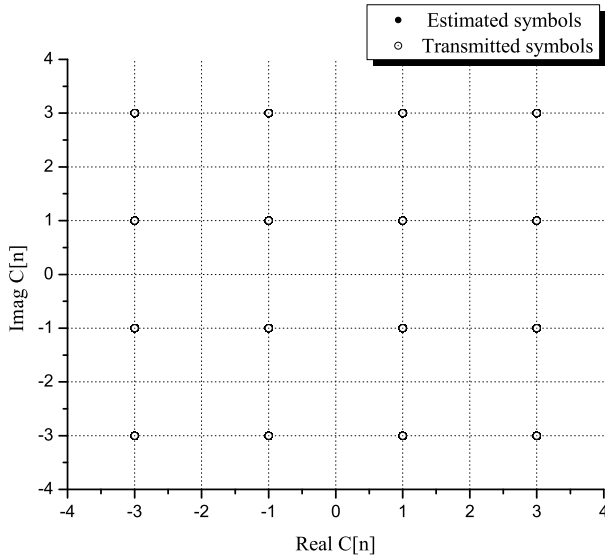

Fig. 10.   Symbol dispersion using DFT interpolation.

It is possible to conclude that the interpolation method influences in the final system performance. Among the three methods previously presented, the DFT interpolation has achieved the best result. On the other hand, this interpolation method is the most complex to be implemented [14].

B. Influence of the delay profile in the channel estimation error and system performance.

The system with parameters shown in Table I has been simulated in two channels with different delay profiles, which are presented in Tables III and IV.

TABLE III
DELAY PROFILE OF CHANNEL 2.

Parameter	P_0	P_1	P_2	P_3	P_4	P_5
Delay [μs]	0	0.15	2.22	3.05	5.86	5.93
Gain [dB]	-0.02	-27	-32	-29	-27	-32

TABLE IV
DELAY PROFILE OF CHANNEL 3.

Parameter	P_0	P_1	P_2	P_3	P_4	P_5
Delay [μs]	0	0.3	3.5	4.4	9.5	12.7
Gain [dB]	0	-12	-4	-7	-15	-22

Table V presents the coherence bandwidth for all channels analyzed in this paper. As it can be seen, the delay profile in Table IV (channel 3) is more severe than the others, resulting in a more frequency-selective channel. The objective of this

TABLE V
COHERENCE BANDWIDTH.

Channel	BW_C - coherence 50%	BW_C - coherence 90%
Channel 1	137.46 kHz	13.74 kHz
Channel 2	617.42 kHz	61.74 kHz
Channel 3	89.84 kHz	8.98 kHz

analysis is to evaluate how the delay profile interferes in the system performance.

The performance of three interpolation methods has been analyzed on channels 2 e 3. The results obtained for each interpolation technique on each channel are shown in Tables VI and VII, respectively.

TABLE VI
RESULTS FOR EACH INTERPOLATION METHOD ON CHANNEL 2.

Interpolation	E_{CE}	MER [dB]
Linear	6.36×10^{-5}	44.76
Cubic	3.80×10^{-5}	49.29
DFT	2.35×10^{-18}	310.97

TABLE VII
RESULTS FOR EACH INTERPOLATION METHOD ON CHANNEL 3.

Interpolation	E_{CE}	MER [dB]
Linear	8.18×10^{-4}	18.13
Cubic	5.89×10^{-4}	20.45
DFT	3.95×10^{-18}	300.29

With these results, one can conclude that the system performance is more degraded on channels with severe delay profiles, which are more frequency-selective. Thus, when the coherence bandwidth is smaller, it is necessary to use more pilot subcarriers in order to prevent the system from being affected by the channel estimation.

C. Influence of the number of pilot subcarriers in the channel estimation and system performance

In this analysis, the number of pilot subcarriers has been reduced to understand how the number of pilot subcarriers interferes in the channel estimation error and in the final system performance. It is important to notice that reducing the number of pilot subcarriers means increasing the frequency spacing between them. In the first simulation iteration the spacing considered between two pilots is 2 subcarriers, which is then increased to $4, 6, 8, 10, 12...200$ subcarries. The E_{CE} and the MER obtained for linear interpolation using the delay profile presented in Table II and the system parameters presented in Table I, except for the number of pilots, are shown in Figure 11 and Figure 12, respectively.

As shown in Figure 11, when the frequency spacing between pilot subcarries increases, i.e., the number of pilots to estimate the channel reduces, the estimation error increases. In Figure 12, when the number of pilots subcarrier decreases, the MER value also decreases but in an exponential way. It must be regarded that in a practical system it is necessary to find
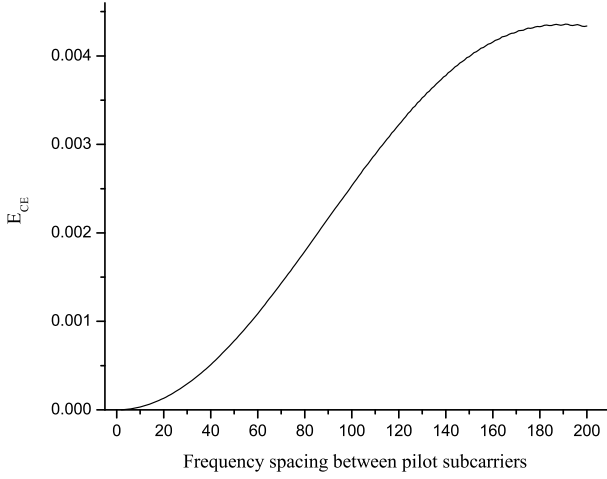
Fig. 11.   Channel estimation error as function of the frequency spacing between pilot subcarriers for linear interpolation.
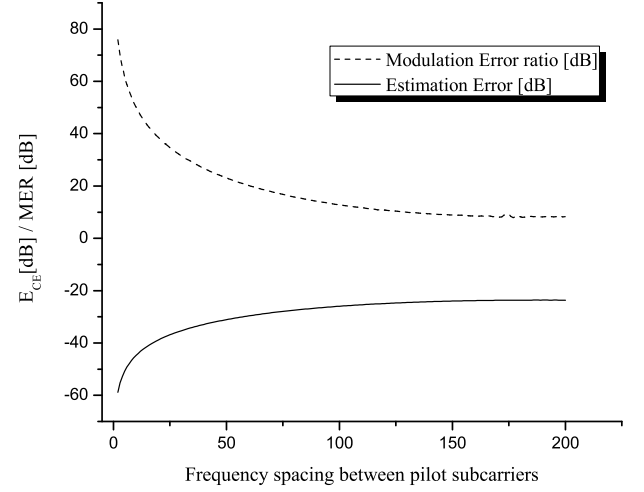
Fig. 12.   Modulation error ratio as function of the frequency spacing between pilot subcarriers for linear interpolation.

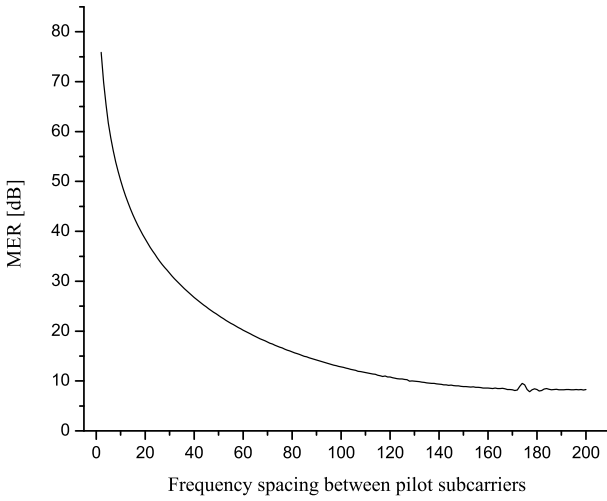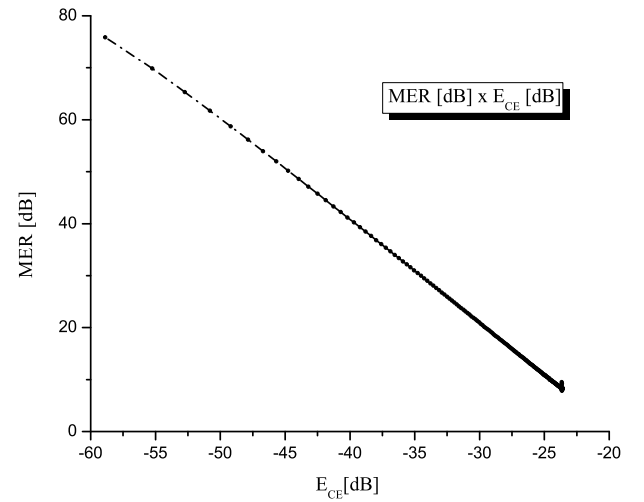Fig. 13.   Channel estimation error and modulation error ratio.

Fig. 14.   MER versus E_{CE} both in dB.

a trade-off between number of subcarriers and E_{CE}, since the increased number of pilot subcarriers reduces system throughput.

One can see that as the channel estimation error increases, the MER of system decreases. However, it is not so easy to establish the exact relationship between these two measures, due to the fact that the MER is expressed in dB and the error is presented in a linear scale.

Figure 13 shows the MER and the channel estimation error, both in logarithmic scale. In this figure, it is more evident how strong the relationship between estimation error and the MER is. When reducing the distance between the pilot subcarriers the estimation error decreases exponentially, while the MER increases exponentially.

Figure 14 presents the MER versus the estimation error, both in logarithmic scale, where it is possible to conclude that the MER is related almost linearly with the channel estimation error, if both measures are analyzed on a logarithmic scale.

Several tests have been performed for the others interpolation methods and others channels with different delay profiles, and the same results have been obtained.

Figure 15 shows the results obtained for all three interpolation methods considered in this paper, where the channel delay profile is described in Table II. As can be seen in Figure 15, the linearity between MER and E_{CE} is maintained for all three interpolation techniques.

The same analysis has been performed for the channel delay profile shown in Table III and the result are presented in Figure 16. The linearity has been maintained and the result was practically the same presented in Figure 15.

The final analysis presented has been performed in the most frequency-selective channel presented, with delay profile shown in Table IV. The results for this channel is shown in Figure 17, where one can also see the linearity between the MER and E_{CE}. However, when the number of pilot subcarriers is reduced there are a region of non-linearity, which is more pronounced in the linear interpolation technique.
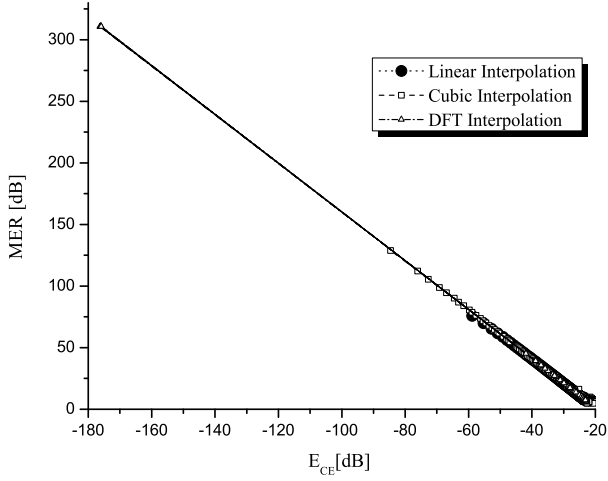
Fig. 15.   MER versus E_{CE} both in dB for all interpolation methods analyzed over channel 1.
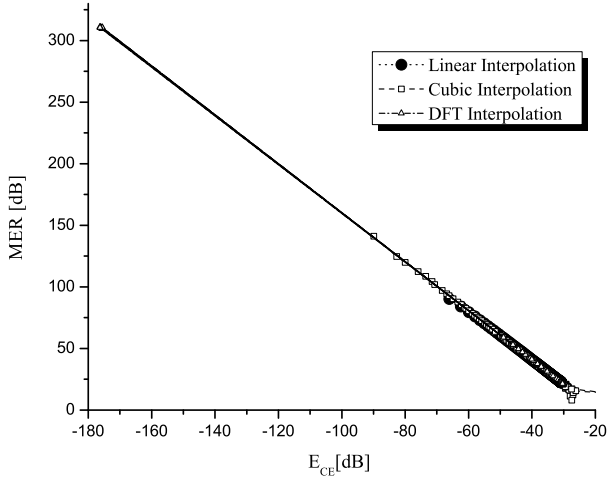

Fig. 16.   MER versus E_{CE} both in dB for all interpolation methods analyzed over channel 2.
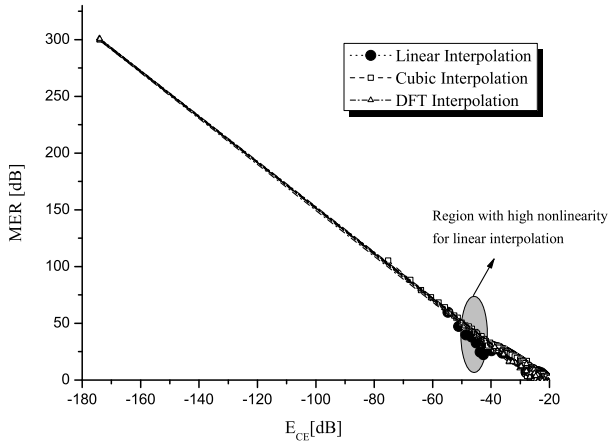

Fig. 17.   MER versus E_{CE} both in dB for all interpolation methods analyzed over channel 3.

The results presented in this paper can be used to derive

a model to estimate the symbol error rate of QAM system considering the channel estimation error. In the final model, it will be possible to estimate the symbol error rate and the corresponding error floor of a M-QAM OFDM with a given RSME.

VI. ANALYZING THE E_{CE} AS AN EQUIVALENT NOISE

Through the presented analysis, it has been showed that each E_{CE} value has a corresponding MER value. Aiming to find an AWGN noise with equivalent effect to a given channel estimation error, which causes a dispersion in the symbol constellation, one must examine the MER parameter.

From (9) it is possible to verify that this parameter is obtained by the ratio between the sum of the symbol energy and the sum of the noise energy. Thus, in order to find the variance of an equivalent noise which causes the same symbol scattering that a given channel estimation error, the MER parameter can be considered as

$$MER = \frac{E}{\sigma_{eq}^2},\qquad(10)$$

where E is the average energy of the transmitted symbols, which in this case is equal to $10J$ (average energy of a 16 QAM constellation) and σ_{eq}^2 represents a AWGN noise variance equivalent to a certain channel estimation error.

In Section V-A, it has been found that for linear interpolation the system achieved a channel estimation error of 3.32×10^{-4} and $MER = 30.7$ [dB]. From (10) the equivalent noise variance, σ_{eq}^2, of $85.0 \times 10^{-4}J$ can be obtained. Figure 18 presents a 16 QAM symbol constellation corrupted by a Gaussian noise with variance $\sigma_{eq}^2 = 85.0 \times 10^{-4}J$.
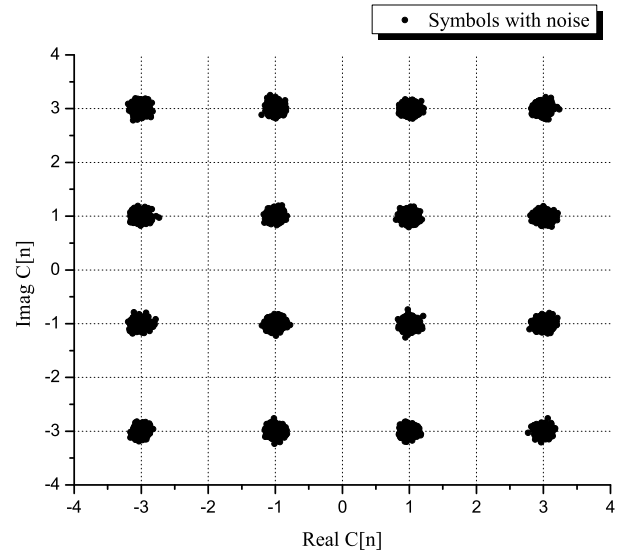

Fig. 18.   Symbol dispersion using the equivalent noise to model the E_{CE}.

Comparing the constellations shown in Figures 18 and 8, it is possible to verify that the symbol dispersion is similar in both cases. Thus, it can be concluded that the model of the

channel estimation error as an AWGN can be used to represent the degradation caused by the channel estimation error.

The same analysis has been done for the cubic interpolation, also shown in section V-A, where $E_{CE} = 5.063 \times 10^{-5}$ and the $MER = 47.1$. The equivalent noise obtained in this case has variance of $\sigma_{eq}{}^2 = 1.95 \times 10^{-4} J$. Figure 19 presents 16 QAM symbol constellation corrupted by an AWGN with $\sigma_{eq}{}^2 = 1.95 \times 10^{-4} J$.
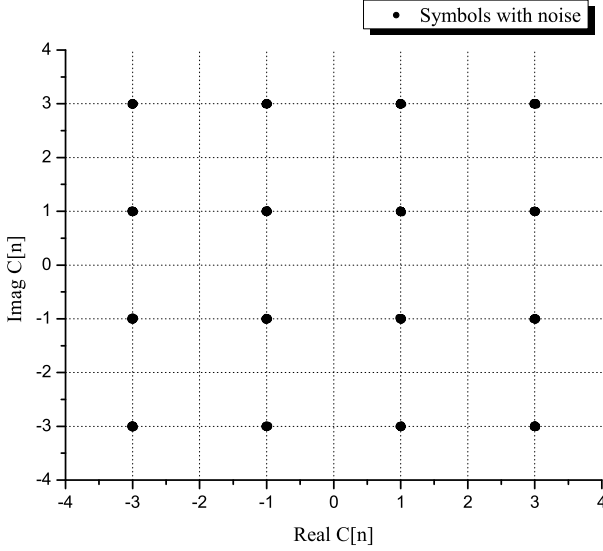

Fig. 19.   Symbol dispersion using the equivalent noise to model the E_{CE}.

The result shown in Figure 19 is also similar to the one shown in Figure 9 and, therefore, validates the proposed model.

As mentioned previously, an expression to estimate the symbol error probability as function of the channel estimation error can be evaluated from the model presented in this paper.

VII. CONCLUSIONS

One challenge in MIMO-OFDM is to perform an accurate channel estimation. This paper has presented some channel estimation techniques that can be used in MIMO-OFDM system that designed for diversity gain. The influence of the interpolation technique on the channel estimation error and the MER has been analyzed. It was also shown how the number of pilot subcarriers impacts on the channel estimation error. Different channels with different delay profiles have also been analyzed. A linear relationship between the channel estimation error and the MER has been found, when both measures are analyzed in a logarithmic scale. This results show that it is possible to model E_{CE} as an equivalent AWGN, which means that this model can be used to estimate the symbol error probability caused by the channel estimation error.

REFERENCES

[1] K. F. Lee, D. B. Willians, "A Space-Time Coded Transmit Diversity Technique For Frequency Selective Fading Channels", *IEEE Sensor Array and Multichannel Signal Processing Workshop*, pp. 149-152, March 2000.

[2] L. Kansal, A. Kansal, K. Singh, "Performance Analysis of MIMO-OFDM System Using QOSTBC Code Structure for M-QAM", *Canadian Journal on Signal Processing*, vol. 2, no. 2, May 2011.

[3] A. Omri, R. Bouallegue, "New Transmission Scheme for MIMO-OFDM System", *International Journal of Next-Generation Networks (IJNGN)*, vol. 3, no. 1, March 2011.

[4] A. R. Bahai, B. R. Saltzberg and M. Ergen, Multi-Carrier Digital Communications: Theory and Applications of OFDM, 2nd ed., Springer, New York, NY, 2004, pp. 1-436.

[5] L. L. Mendes, "Modelos Matemáticos para Estimação do Desempenho de Sistemas de Multiplexação por Divisão em Frequências Ortogonais", Ph.D. dissertation, Dept. Elect. Eng., UNICAMP, Campinas, SP, Brazil, 2007.

[6] A. J. Paulraj, D. A. Gore, R. U. Nabar, H. Bolcskey, "An Overview of MIMO Communications - A Key to Gigabit Wireless", *Proceedings of the IEEE*, vol. 92, no. 2, February 2004.

[7] S. Alamouti, "A Simple Transmit Diversity Technique for Wireless Communications", *IEEE Journal on Select Areas on Communications*, vol. 16, no. 8, pp. 1451-1458. October 1998.

[8] H. Bolcskei, D. Gesbert, A. J. Paulraj, "On the Capacity of OFDM-Based Spatial Multiplexing Systems", *IEEE Transactions on Communications*, vol. 50, no. 2, February 2002.

[9] W. C. Freitas Jr., F. R. P. Cavalcanti, R. R. Lopes, "Hybrid MIMO Transceiver Scheme With Antenna Allocation and Partial CSI at Transmitter Side", *International Journal of Computer Technology and Electronics Engineering (IJCTEE)*, vol. 1, no. 2, pp. 104-108. February 2012.

[10] M. Agrawal, Y. Raut, "Effect of Guard Period Insertion in MIMO OFDM System", *IEEE Transactions on Communications*, vol. 50, no. 2, February 2002.

[11] D. C. Moreira, "Estratégias de Estimação de Canal para Adaptação de Enlace em Sitemas MIMO-OFDM", M.S. thesis, UFC, Fortaleza, CE, Brazil, 2006.

[12] R. G. Trentin, "Técnicas de Processamento MIMO-OFDM Aplicadas à Radiodifusão de Televisão Digital Terrestre.", M.S. thesis, UFSC, SC, Brazil, 2006.

[13] E. Manasseh, S. Ohno, M. Nakamoto, "Combined Channel Estimation and PAPR Reduction Technique for MIMO-OFDM Systems With Null Subcarriers", *EURASIP Journal on Wireless Communications and Networking*, 2012.

[14] L. L. Mendes, R. Baldini, "On Performance of Channel Estimation Algorithms for STC-OFDM Systems in Non-linear Channels", *"10th International Symposium on Communication Theory and Application"*, 2009.

[15] O. Simeone, Y. Bar-Ness, U. Spagnolini, "Pilot-Based Channel Estimation for OFDM Systems by Tracking the Delay-Subspace", *IEEE Transactions on Wireless Communications*, vol. 3, no. 1. January 2004.

[16] S. Coleri, M. Ergen, A. Puri, A. R. Bahai, "Chanel Estimation Techniques Based on Pilot Arrangement in OFDM Systems", *IEEE Transactions on Broadcasting*, vol. 48, no. 3, pp. 223-229. September 2002.